Elastic properties of β−SiC films by Brillouin light scattering

ARTICLE *in* JOURNAL OF APPLIED PHYSICS · FEBRUARY 2004

Impact Factor: 2.18 · DOI: 10.1063/1.1642281

Elastic properties of β-SiC films by Brillouin light scattering

Philippe Djemia,[a] Yves Roussigné, and Guy F. Dirras
Laboratoire des Propriétés Mécaniques et Thermodynamiques des Matériaux, UPR CNRS 9001, Université Paris Nord, Avenue J.B. Clément, 93430 Villetaneuse, France

Kamili M. Jackson
Department of Mechanical Engineering, The Johns Hopkins University, 3400 N. Charles Street, Baltimore, Maryland 21218

(Received 23 September 2003; accepted 25 November 2003)

Brillouin light scattering has been used to investigate elastic properties of a monocrystalline and of ⟨111⟩ textured polycrystalline 3C polytype silicon carbide films that have been deposited on silicon substrate by chemical vapor deposition. Taking advantage from the detection of different acoustic modes, a complete elastic characterization of the films has been achieved. The three unknown elastic constants of the monocrystalline 3C-SiC, namely, $c_{11}=395$ GPa, $(c_{11}-c_{12})/2=136$ GPa, and $c_{44}=236$ GPa have been selectively determined, respectively, from the frequency of the longitudinal and of the shear horizontal bulk modes traveling parallelly to the film surface. These determinations are in agreement with the frequency of the observed Rayleigh surface mode, of the pseudosurface mode, and of the bulk waves propagating at different angles from the normal of the single crystal film plane and consistent with existing theoretical calculations of β-SiC elastic constants. Finally, the calculated Voigt average values of the effective elastic constants for the ⟨111⟩ textured 3C-SiC polycrystalline film using the single crystal constants provides a good agreement with our experimental results ($C_{11}=500$ GPa, $C_{33}=535$ GPa, $C_{44}=165$ GPa, $C_{66}=210$ GPa, and $C_{13}=50$ GPa) and compare fairly well with the α-SiC published one. These results confirm that the elastic constants of silicon carbide are slightly influenced by the polytypism. © *2004 American Institute of Physics.* [DOI: 10.1063/1.1642281]

I. INTRODUCTION

The determination of the mechanical properties, specifically elastic properties of thin layers deposited on a substrate is important for both physical models and engineering application purposes. Indeed, a lot is known about the elastic properties of bulk materials but in most cases, information concerning thin films is scarce and sometimes unreliable. This is mainly due to the difficulties in measuring such properties with appropriate and accurate tools, although the deposition and the structural characterization techniques have significantly progressed during the last few years, providing for better materials with an improved knowledge of their microstructure. Nowadays, there are only a few widely used techniques for such mechanical measurements, namely, the surface Brillouin light scattering (BLS),[1] the picosecond ultrasonics,[2] the Bulge/Blister test,[3] the vibrating reed device,[4] the nano-indentation,[5] and microtensile tests.[6,7] Most of the time, one needs to use a combination of these techniques in order to fully determine their elastic constants or moduli.

Silicon carbide (SiC) exhibits a form of one-dimensional polymorphism called polytypism. SiC crystallizes in many different polytypes, which differ from one another only in the stacking sequence of a double layer. Each double layer consists of two planes of close-packed Si and C atoms (one Si atom lying directly over one C atom), and each successive double layer is stacked over the previous one in a close-packed arrangement. The two most common SiC polytypes are the 3C-SiC and 6H-SiC. The 3C polytype, also known as β-SiC, is the only polytype with a cubic structure. In addition to 3C-SiC, about 70 hexagonal (among them 6H-SiC) and 170 rhombohedral crystal structure arrangements are possible. They are known as α-SiC. SiC has long been recognized as a semiconductor material with outstanding physical and chemical characteristics. Compared to Si, SiC exhibits a larger band gap, a higher breakdown field, and a higher thermal conductivity. These properties make SiC very attractive for the fabrication of high-temperature, high-power, and high-frequency electronic devices. In addition, its favorable mechanical properties such as high elastic modulus and a fracture toughness higher than for Si, in combination with its large band gap, make SiC an excellent material for the fabrication of microsensors that can operate at temperatures higher than 600 °C. Compared to Si, SiC has demonstrated higher chemical inertness and radiation resistance which also increases its potential for sensors operating in harsh environments. Historically, most research has focused on developing 6H-SiC as a semiconductor material for high-temperature and high-power electronics. But small wafer size and the inability to grow epitaxial layers on any substrates other than 6H-SiC has hindered the development of the 6H polytype. Over the last decade, however, there has been growing interest in 3C-SiC as a microelectromechanical systems (MEMS) material. Unlike 6H-SiC, the 3C polytype can be epitaxially grown on single-crystal silicon substrates. At Case Western

[a]Electronic mail: djemia@lpmtm.univ-paris13.fr

Reserve University (CWRU), the first successful depositions of spatially uniform, single-crystal, 3C-SiC films on 4 in. (100) single-crystal silicon wafers have been achieved. These epitaxial 3C-SiC films are well suited for bulk micromachined structures like diaphragms and cantilever beams, since SiC films are highly resistant to KOH and EDP etching. For such films, surface micromachining is not possible so that poly-SiC has to be grown on an appropriate sacrificial layer on silicon.

To better understand the intrinsic thermomechanical properties of SiC thin films, we have studied in detail some mechanical and structural aspects of two cubic 3C-SiC films: monocrystalline and ⟨111⟩ fiber-textured polycrystalline films with thickness in the micrometer range. Previous BLS studies dealt with bulk α-SiC single crystal of two polytype 4H and 6H (Ref. 8) of hexagonal symmetry. In this article, the elastic properties are studied in relation to the texture of the films. The experimental investigations have been carried out using x-ray diffraction and a BLS technique which has proven to be a powerful nondestructive tool for the elastic characterization of layered structures.[1] The three independent elastic constants of the β-SiC epitaxial film are selectively determined from the analysis of a number of different surface acoustic modes traveling in the (001) plane along various in-plane crystallographic directions. A further check is made by the analysis of the observed bulk modes, allowing the derivation of the refractive index for the 514.5 nm radiation wavelength. Finally, the calculated Voigt average values of the effective elastic constants for the ⟨111⟩ textured polycrystalline using the determined single crystal constants provides a good agreement with the ones derived from the analysis of our Brillouin light scattering experiments.

II. BRILLOUIN LIGHT SCATTERING TECHNIQUE

In a BLS experiment, a beam of monochromatic light is used as a probe to reveal acoustic phonons that are naturally present in the medium under investigation. The power spectrum of these excitations is mapped out from frequency analysis of the light scattered within a solid angle, by means of a multipass Fabry–Perot interferometer. A number of acoustic modes confined within the film material can thus be revealed, and the elastic constants of the film determined.[9–11]

The Brillouin experiments were performed at room temperature. The light source is an Ar^+ laser tuned on a 514.5 nm single mode line. Incident 100–500 mW *p*-polarized light is focused on the surface of the sample. The scattered light is analyzed by means of a Sandercock-type 3+3 pass tandem Fabry–Perot interferometer. For some spectra, an analyzer was inserted within the path of scattered light providing the *s*- or *p*-polarized part of the spectra. The typical duration for the acquisition of a Brillouin spectrum was 2–4 h. For a transparent film a few microns thick, deposited on an opaque substrate, two different geometries of interaction contribute to the inelastic scattering of light from acoustic phonons in the film,[10] as shown in the schematic wave vector diagram of Fig. 1. In the present work we used the backscattering geometry. In this condition the wave vector of the involved surface phonons propagating along the surface is determined by the relation

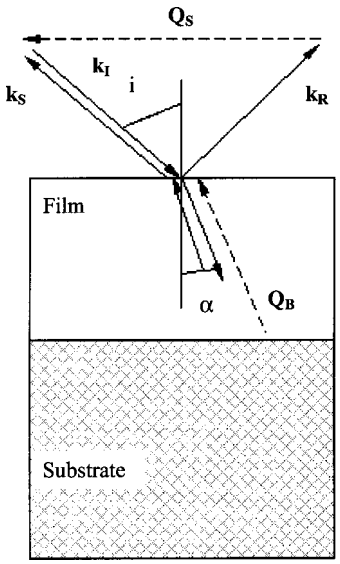

FIG. 1. Schematic diagram of interaction between photons and phonons, in the backscattering geometry. Here $\mathbf{k_I}$, $\mathbf{k_S}$, and $\mathbf{k_R}$ are the wave vector of incident, scattered, and reflected photons, respectively, while $\mathbf{Q_B}$ and $\mathbf{Q_S}$ are those of bulk and surface phonons, respectively.

$$Q_S = 2k_I \sin(i), \tag{1}$$

where k_I denotes the optical wave vector in air and where i is the angle of incidence. The wavelength of the surface phonons probed in this experiment are around 300 nm. The velocity (v_S) is deduced from the measured frequency (Ω) by the relation

$$v_s = \Omega / Q_S . \tag{2}$$

The wave vector of the involved bulk phonons is experimentally adjusted to the value

$$Q_B = 2nk_I , \tag{3}$$

where n is the refractive index of the film corresponding to the propagation direction of light inside the film (isotropic for materials of cubic symmetry). The velocity (v_B) is deduced from the measured frequency (Ω) by the relation

$$v_B = \Omega / Q_B . \tag{4}$$

III. SAMPLE PREPARATION AND STRUCTURAL CHARACTERIZATIONS

The epitaxial 3C-SiC film with thickness in the micrometer range was fabricated in the Microfabrication Laboratory at CWRU using an atmospheric pressure chemical vapor deposition (APCVD) system. A 50 kW rf generator with a ten turn induction coil is used to heat the susceptor. The process gases were propane (15% hydrogen) and silane (5% hydrogen). The three-step deposition process begins with an *in situ* hydrogen etch, followed by the formation of a carbonized layer on the substrate surface and film growth. Prior to deposition, the chamber is pumped down to below 100 mTorr, then backfilled to atmospheric pressure with ultrahigh purity argon. A series of pump/purge cycles are performed to

flush the chamber of gaseous contaminants. Following the final purge, hydrogen is introduced into the chamber. Upon complete displacement of argon by hydrogen, the susceptor is heated from room temperature to 1000 °C and is held constant for a few minutes. During this step, hydrogen etches the polysilicon native oxide, as well as any metallic and organic contaminants from the polysilicon surface. After the hydrogen etch, the susceptor is then cooled to below 500 °C. The carbonization process is then initiated by heating the susceptor to 1360 °C under a stable flow of propane and hydrogen. Once the temperature reaches 1360 °C, temperature and flow rates are constant for several seconds. During this step, propane breaks into hydrocarbon fragments as it passes over the heated susceptor. As these fragments are absorbed on the substrate, they react with silicon at the surface, forming SiC. The reaction will continue until a thin film of poly-SiC is grown, after which Si from the substrate can no longer reach the absorbed carbon and growth ceases. Simultaneously reducing the propane flow and introducing silane film growth continues. Ceasing the flow of propane and silane, and then cooling the susceptor under hydrogen flow terminates film growth. The polycrystalline sample with thickness in the micrometer range was fabricated at Massachusetts Institute of Technology (MIT) by chemical vapor deposition. The process gases were CH_3SiCl_3 and hydrogen and the temperature range was 1000–1300 °C.

X-ray diffraction measurements have been performed with a four circles goniometer (INEL) using a cobalt anode. A predominant ⟨111⟩ fiber texture was found for the MIT polycrystalline film whereas the 3C-SiC films showed a ⟨001⟩ out of plane orientation (see Refs. 12 and 13).

IV. RESULTS AND DISCUSSION

The Brillouin spectra have been analyzed using a Green function approach of the equations of elasticity, with appropriate boundary conditions, in order to evaluate the spectral density of the displacements $u_z(z=0)$, $u_y(z=0)$, and $u_x(z=0)$ at the free surface,[9] which are relevant for the frequency position of the lines observed in Brillouin scattering spectra from surface acoustic waves. The x axis is along the propagation wave vector in the plane of the film and the z axis along the normal to the film plane.

A. The CWRU epitaxial film

The analysis of the surface waves for various directions of propagation from the [100] to the [110] axis enables us to measure unambiguously the three independent single crystal elastic constants of the epitaxial film.

In Fig. 2, we show spectra for four directions of propagation referred to the angle denoted ϕ which is measured from the [010] axis to the [100] axis in the (001) plane. These spectra were obtained at an angle of incidence $i=45°$ with no polarization of the analyzed scattered electric field. The peaks labeled RW, PSM, SHM, and HFPSM correspond, respectively, to the generalized Rayleigh surface wave, the pseudosurface mode, the shear horizontal mode, and the high-frequency pseudosurface mode, traveling parallelly (or nearly parallelly for the pseudosurface modes) to the film surface. RW has a sagittal polarization only for the ⟨100⟩ high symmetry directions, HFPSM has a longitudinal character, and SHM a quasishear horizontal polarization. PSM is a leaky wave that propagates nearly parallel to the surface and exists only for some planes of anisotropic material over a finite range of propagation directions (in our case above $\phi \approx 25°$) and has a velocity higher than the bulk SHM mode. All these lines are reproduced in the relevant power spectrum of the displacement field components: u_x, u_y, and u_z calculated at the free surface (see Fig. 2).

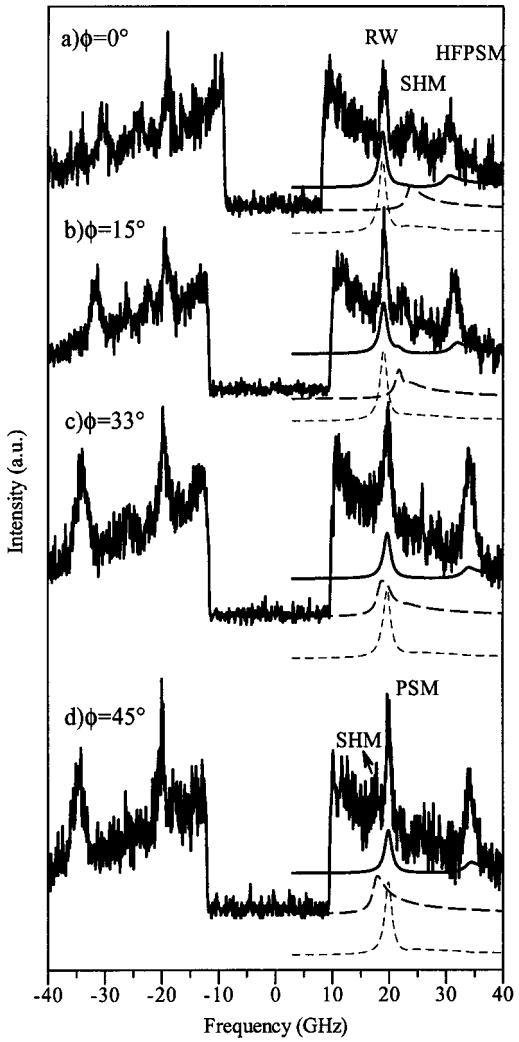

FIG. 2. Brillouin spectra obtained from the epitaxial silicon carbide film for various directions of the wave vector of the surface acoustic waves referred to the angle denoted ϕ which is measured from the [010] axis to the [100] axis in the (001) plane. The angle of incidence is $i=45°$. The peaks labeled RW, PSM, SHM, and HFPSM correspond, respectively, to the generalized Rayleigh surface wave, the pseudosurface mode, the shear horizontal mode, and the high-frequency pseudosurface mode, traveling parallel (or nearly parallel for the pseudosurface modes) to the film surface. We show also for comparison the calculated power spectrum for the related component (full thick line) u_x, (medium dotted line) u_y, and (thin dotted line) u_z of the displacement field, at the free surface.

The measurements of the frequency position of these Brillouin peaks provide the phase velocity v of the corresponding acoustic modes, according to Eq. (2). Notice that the phase velocity of the HFPSM is $\sqrt{c_{11}/\rho}$ (propagation along ⟨010⟩) and $\sqrt{(c_{11}+c_{12}+2c_{44})/2\rho}$ (propagation along ⟨110⟩), so that c_{11} can be directly determined from the first

TABLE I. Measured velocity v of the surface acoustic waves in the (001) plane of the monocrystalline 3C-SiC film for propagation along the [100] and [110] high symmetry directions with their related elastic constants ρv^2 (the mass density is assumed to be 3.21 g/cm^3).

	v_R (km/s) along [100]	v_{PSM} (km/s) along [110]	v_{SHM} (km/s) along [100]	v_{HPSM} (km/s) along [100]	v_{SHM} (km/s) along [110]	v_{HFPSM} (km/s) along [110]
Velocity	6.94±0.05	7.27±0.15	8.59±0.16	11.11±0.18	6.51±0.2	12.53±0.19
	c_R	c_{PSM}	c_{44}	c_{11}	$(c_{11}-c_{12})/2$	$(c_{11}+c_{12}+2c_{44})/2$
Elastic constant (Gpa)	154±2	170±7	236±7	395±12	136±8	504±15

relation, using $\rho=3.21$ g/cm^3 for the mass density. As for the RW, its velocity is $\beta\sqrt{c_{44}/\rho}$ (propagation along $\langle 010\rangle$), where β is only weakly dependent on c_{11} and c_{12}. RW degenerates with the SHM mode for propagation direction along $\langle 110\rangle$. The phase velocity of SHM is simply, $\sqrt{c_{44}/\rho}$ (propagation along $\langle 010\rangle$) and $\sqrt{(c_{11}-c_{12})/2\rho}$ (propagation along $\langle 110\rangle$). Thus c_{44} and $(c_{11}-c_{12})/2$ can also be selectively determined. The measured velocity data of the surface acoustic waves for the high symmetry directions [100] and [110] are reported in Table I with their related elastic constants. The four independent relations provided by the shear horizontal mode and by the high-frequency pseudosurface mode for the two high symmetry directions allow the determination of the three independent elastic constants c_{11}, c_{12}, and c_{44} that are reported in Table II. As the elastic constant c_{12} can be obtained either by using the relation in column five ($c_{12}=123$ GPa) or six ($c_{12}=141$ GPa) in Table I with c_{11} and/or c_{44} as input, we take the average between these two values ($c_{12}=132\pm9$ GPa). These measured single crystal constants are in fairly good agreement with previous theoretical determination and some partial experimental results like the bulk modulus [we found $B=(c_{11}+2c_{12})/3=219$ GPa] or sound velocities measurements.[14–17] Furthermore, we show in Fig. 3 the evolution of the calculated velocities of the surface modes for various in plane directions of propagation compared to the experimental measurements. This demonstrates the in plane cubic anisotropy and the perfect agreement of the fit for the entire range of direction of propagation. PSM exists for propagation directions at an angle ϕ higher than around 25°. For $\phi=45°$ the Rayleigh surface wave degenerates with the SHM.

In addition to the analysis of the surface waves, we have also investigated the Brillouin spectra of the bulk waves that propagate almost normally to the surface of the film, see, for example, Fig. 4. The peaks at larger frequency in the spectrum of Fig. 4 correspond to the bulk shear wave (BSW) and to the bulk longitudinal acoustic wave (BLW) observed for an angle of incidence of the light $i=65°$ (it corresponds to a propagation of these waves nearly normal to the surface inside the film). Different from the previous case, the interaction geometry here is relative to bulk phonons whose wave vector is expressed by Eq. (3) while the velocity is given by Eq. (4). Due to refraction at the air/film interface, the bulk waves associated with the BLW and BSW peaks have a wave vector at an angle:

$$\alpha=\sin^{-1}[\sin(i)/n] \tag{5}$$

from the surface normal. For $\alpha=0°$ (propagation normal to the film plane) the BLW phase velocity is simply $\sqrt{c_{33}/\rho}$ (with $c_{33}=c_{11}$ for the considered cubic symmetry), while the phase velocity of the shear mode BSW is $\sqrt{c_{44}/\rho}$. For an increased α angle, their phase velocity depends also on c_{11} and c_{12}. Measurements of the bulk wave velocities were performed from orthogonal incidence to a larger angle. As all the elastic constants are known, the previous determination is checked once more from the surface mode analysis and the

TABLE II. Experimental values of the three independent elastic constants of the 3C-SiC single crystal (c_{11}, c_{12}, c_{44}) and of the five independent effective elastic constants of the polycrystalline sample analyzed in the present work (C_{11}, C_{33}, C_{44}, C_{66}, C_{13}). The Voigt and Reuss estimated values of the elastic constants for a $\langle 111\rangle$ textured polycrystalline silicon carbide using for calculations the single crystal values are also reported for comparison in the last line (inside the square brackets). The experimental values for 4H- and 6H-SiC bulk single crystals determined by Kamitani *et al.* (Ref. 8) are reported in the last line.

	C_{11}(GPa)		C_{44}(GPa)		C_{12}(GPa)
Single crystal	395±12		236±7		132±9
	C_{11}(GPa)	C_{33}(GPa)	C_{44}(GPa)	C_{66}(GPa)	C_{13}(GPa)
Polycrystal	500±30	535±10	165±10	210±10	50
$\langle 111\rangle$ textured polycrystalline 3C-SiC	500[485]	534[534]	166[154]	201[187]	62[62]
4H and 6H bulk single crystal	501±4	553±4	163±4	195±5	52±9

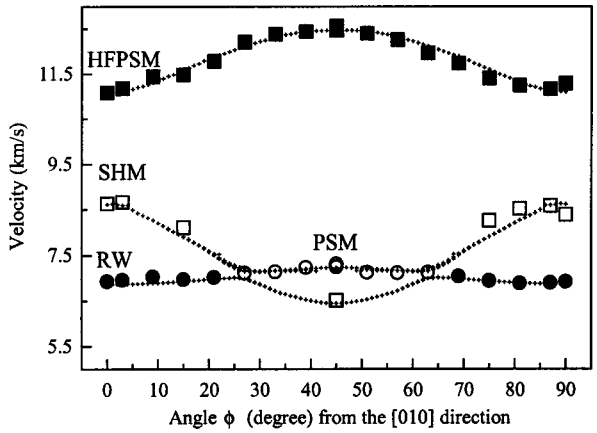

FIG. 3. Evolution of the calculated (small cross) and of the experimental velocity of the surface acoustic waves in the (001) plane. The direction of propagation is repered from the [010] direction. RW (closed dots), SHM (open squares), HFPSM (closed squares), and PSM (open dots) denote, respectively, the Rayleigh wave, the (quasi) shear horizontal wave, the high-frequency pseudosurface mode, and the pseudosurface mode.

refractive index of the epitaxial SiC film is determined as $n=3.22\pm0.03$ for the radiation wavelength of 514.5 nm, used here.

The elastic constants of the epitaxial 3C-SiC film as listed in Table II yield the Zener ratio $A=2c_{44}/(c_{11}-c_{12})=1.79$ and the anisotropy parameter $S=s_{11}-s_{12}-s_{44}/2=1/(c_{11}-c_{12})-1/2c_{44}=0.0015\ \mathrm{GPa}^{-1}$ (see Ref. 18). It follows that the epitaxial film is elastically anisotropic (elastic isotropy in cubic crystals is $A=1$). As a consequence, directionality equations must be used to describe Young's modulus as well as the two Poisson ratios. It should be reminded that given a crystallographic plane and a longitudinal stress within that plane, orthogonal strains may vary depending on the direction; the definition of Poisson's ratio must therefore be extended in the sense that ν refers to the longitudinally induced orthogonal strain whereas ν' refers to the transversely induced strain. A convenient way of visualizing the

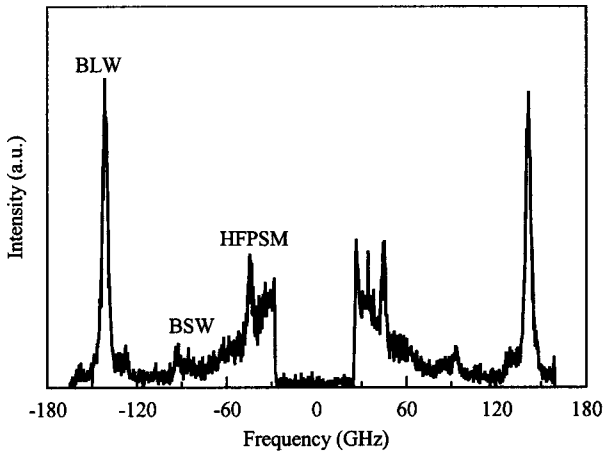

FIG. 4. Experimental spectrum obtained (p incident light – np scattered light geometry) for the epitaxial silicon carbide film and a propagation wave vector in the (100) plane, at larger frequency with an angle of incidence $i=65°$ corresponding to $\alpha=16°$. BLW and BSW denote, respectively, the bulk longitudinal wave and the bulk shear wave.

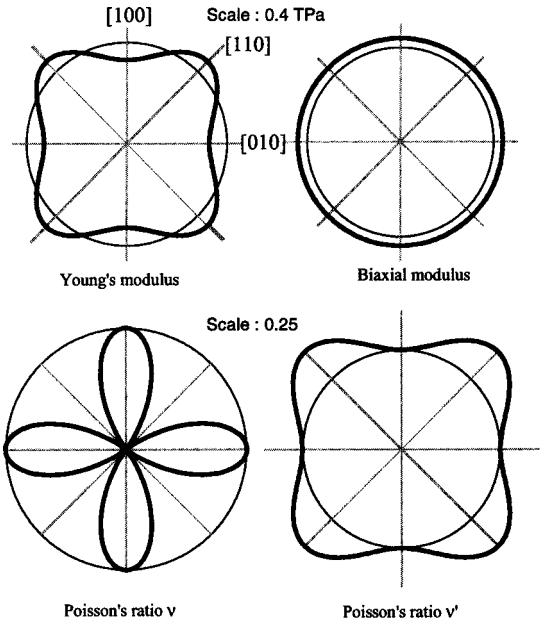

FIG. 5. Rotational dependence of the Young's modulus, the biaxial modulus, and the two Poisson's ratios of the single-crystal 3C-SiC film for applied stresses within {100} planes. Poisson's ratio ν refers to a longitudinal orthogonal elongation, whereas ν' refers to a transverse orthogonal elongation.

directionality then consists on focusing attention on a specific crystallographic plane and examining the variations in E, ν, and ν' in that plane. By choosing a proper set of reference planes, the directionality thus can be assessed. In that context, for crystallographic planes identified by Miller indices (hkl), one can derive the equations[19]

$$E_{(hkl)}=\left(s_{12}+\frac{s_{44}}{2}+S\Omega_{22}\right)^{-1},$$
$$\nu_{(hkl)}=-(s_{12}+S\Omega_{23})E_{(hkl)}, \tag{6}$$
$$\nu'_{(hkl)}=-(s_{12}+S\Omega_{12})E_{(hkl)},$$

where the Ω_{ij} are functions of (i) the two Eulerian angles of the plane under consideration and (ii) the angle θ that specifies a direction in the plane. These directionality functions reduce to the following expressions for the (001) plane[19]

$$\Omega_{12}=0,$$
$$\Omega_{22}=\frac{3}{4}+\frac{1}{4}\cos(4\theta), \tag{7}$$
$$\Omega_{23}=\frac{1}{4}-\frac{1}{4}\cos(4\theta).$$

The angle θ must be measured from the principal axes $\langle100\rangle$. The rotational dependence of these elastic moduli is shown in Fig. 5 with the in plane biaxial modulus $E/(1-\nu)$, which relates longitudinal stresses and strains and frequently emerges in a situation of practical interest (bulge test method, thermal stresses, ...). This modulus is isotropic in the {100} orientation. The two ratios ν and ν' differ substantially except for principal stress directions where they are equal to 0.25. The higher values of E and ν' are obtained for a lon-

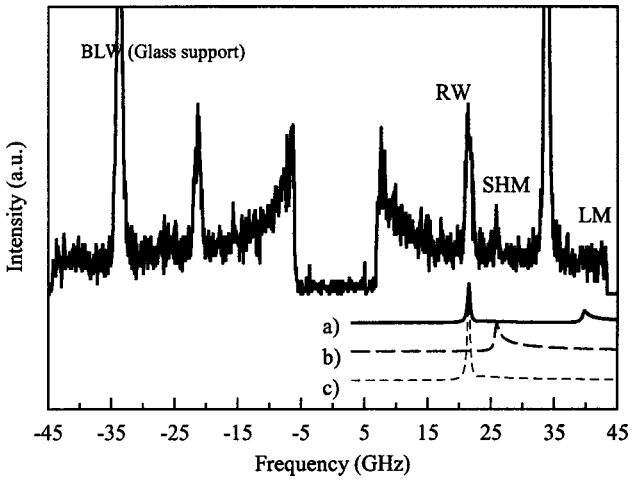

FIG. 6. Experimental spectrum obtained for the self-supported polycrystalline silicon carbide fixed on a float-glass plate, for an angle of incidence equal to 55°. RW, SHM, and LM denote, respectively, the Rayleigh wave, the shear horizontal wave, and the longitudinal mode. Below, we show also for comparison the calculated power spectrum for the related component u_x (bold line), u_y (dash line), and u_z (dotted line) of the displacement field, at the free surface.

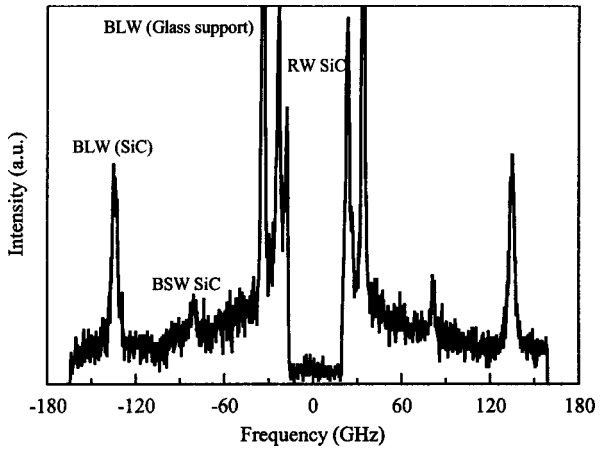

FIG. 7. Experimental spectrum obtained (p incident light – np scattered light geometry) for the self-supported polycrystalline silicon carbide fixed on a float-glass plate, at larger frequency with an angle of incidence $i=65°$ corresponding to $\alpha=19°$.

gitudinal stress applied along the direction [110] and is, respectively, 455 ± 10 GPa and 0.34 ± 0.03. This value of the Young modulus for this orientation compares well with the one measured by the interferometric strain displacement gage (ISDG) method[12,13] which was found to be 420 ± 45 GPa.

B. The MIT polycrystalline film

For the polycrystalline sample with hexagonal effective symmetry, the analysis of the surface waves gives access to some effective elastic constants of the films. The remaining ones are obtained by analyzing the revealed bulk modes thanks to the strong photoelastic coupling inside the film and to the reflecting film/substrate interface. In Fig. 6, we show a spectrum taken at an angle of incidence $i=45°$. The two peaks labeled RW and LM correspond, respectively, to the Rayleigh surface wave and to the longitudinal mode, traveling parallel to the film surface.[20] The Rayleigh wave has a sagittal polarization and LM a longitudinal character. Measurements of the frequency position of these two Brillouin peaks enabled us to determine the phase velocity v of the corresponding acoustic modes, according to Eq. (2). Notice that the phase velocity of LM is $\sqrt{C_{11}/\rho}$, so that C_{11} can be directly determined, using for the mass density the value in Table I. As for the RW, its velocity is $\beta\sqrt{C_{44}/\rho}$, where β is only weakly dependent on C_{11}, C_{13}, and C_{33} in the case of the hexagonal symmetry. Because of the large film thickness, the remaining peak labeled SHM corresponds to a shear horizontal mode traveling parallel to the film surface, and its phase velocity is simply, $\sqrt{C_{66}/\rho}$. Due to the large film thickness and to the presence of the reflecting interface, the SHM appears as a well-defined peak in the spectrum. This provides a direct evaluation of C_{66} that is usually very difficult because of the very low scattering efficiency of shear horizontal modes. All these lines are reproduced in the relevant power spectrum of the displacement field components: u_x, u_y, and u_z calculated at the free surface [see Figs. 6(a)–6(c)]. The peaks at larger frequency in the spectrum of Fig. 7 correspond to the bulk shear wave (BSW) and to the bulk longitudinal acoustic wave (BLW) observed for an angle of incidence $i=65°$. Different from the previous case, the interaction geometry is relative here to bulk phonons whose wave vector is expressed by Eq. (3) while the phase velocity is given by Eq. (4). We notice that BLW and BSW peaks are broadened because the interaction volume is limited by the finite thickness of the films.[21] For $\alpha=0°$ the BLW phase velocity is simply $\sqrt{C_{33}/\rho}$, while the shear mode BSW one is $\sqrt{C_{44}/\rho}$. For an increased α angle, their phase velocity depends also on C_{11}, C_{13}, and C_{44}.[10] Measurements of the bulk waves' velocities were performed from orthogonal incidence to a larger angle. A best fit procedure of the BLW, BSW, and RW experimental data to the calculated phase velocities of the corresponding modes leads to the determination of C_{33}, C_{13}, and C_{44}. The refractive index was found to be different from that of the single crystal and equal to 2.75 ± 0.03. The experimental values of the elastic constants are shown in Table II. For comparison purposes, the calculated values of the elastic constants of polycrystalline silicon carbide with ⟨111⟩ fiber texture following a Voigt and Reuss averaging procedure[22] are also reported. A closed agreement is found with our experimental results and those of Ref. 8 for 4H and 6H single crystals. These results confirm, as it was already suggested, that considering the hexagonal symmetry, the elastic constants of silicon carbide are slightly dependent of the polytypism.[23,24] Our results show also that the bulk modulus $B=(C_{11}+2C_{12})/3=219$ GPa is invariant regarding the film crystallography (single crystalline or polycrystalline). The elastic moduli and the Poisson's coefficient can be calculated through well-known relations.[10] The value of the Young modulus E and of the Poisson ratio ν' is found to be, respectively, 485 ± 15 GPa and 0.15 ± 0.01. The value of the Young modulus compares well with the one measured experimentally by the ISDG method[12,13] which was found to be 430 ± 40 GPa.

V. SUMMARY AND CONCLUSION

We have determined using Brillouin light scattering the mechanical properties of a monocrystalline and of a ⟨111⟩ textured polycrystalline cubic polytype 3C silicon carbide in the thickness range of a few microns, which is typical of many applications. The films were grown by chemical vapor deposition on a silicon substrate and characterized by x-ray diffraction. The three independent radiocrystallographic elastic constants c_{11}, c_{12}, and c_{44} of the monocrystalline 3C-SiC film and the five independent effective elastic constants of the ⟨111⟩ fiber-textured polycrystalline film have been successfully measured. The c_{11}, c_{12}, and c_{44} constants were derived from four independent relations taking advantage of the in plane cubic anisotropy. The effective elastic constants of the polycrystalline sample C_{11} and C_{66} were directly obtained from measurements of the phase velocity of the longitudinal and of the shear horizontal modes propagating along the surface in the film material. The remaining constants C_{13}, C_{33}, and C_{44} were evaluated from measurements of the phase velocity of the bulk longitudinal and shear acoustic waves for different propagation directions from the normal of the film plane, and of the Rayleigh surface wave.

The measured single crystal constants are in fairly good agreement with previous theoretical determination and some partial experimental results like the bulk modulus (we found $B=219$ GPa) or sound velocities measurements.[14–17] The values of the measured elastic constants of the polycrystalline film compare fairly well with those calculated using the Voigt or Reuss average procedure for a ⟨111⟩ oriented cubic polycrystalline material, using the determined single crystal elastic constants and with those of 4H and 6H single crystals.[8] These results confirm as it was already suggested that the elastic constants of silicon carbide are slightly dependent of the polytypism.

ACKNOWLEDGMENTS

Dr. K. M. Jackson wishes to thank Professor Chris Zorman at CWRU and Professor Mark Spearing at MIT for providing SiC films studied in this work.

[1] F. Nizzoli and J. R. Sandercock, *Dynamical Properties of Solids*, edited by G. K. Horton and A. A. Maradudin (Elsevier Science, North Holland, Amsterdam, 1990).
[2] C. Thomsen, H. T. Grahn, H. J. Maris, and J. Tauc, Phys. Rev. B **34**, 4129 (1986).
[3] G. E. Heinen and J. E. Hilliard, J. Appl. Phys. **54**, 728 (1983).
[4] C. M. Su and M. Wuttig, J. Alloys Compd. **211/212**, 428 (1994).
[5] J. Woirgard and J. C. Dargenton, Meas. Sci. Technol. **6**, 16 (1995).
[6] W. Sharpe, Jr., Mater. Res. Soc. Symp. Proc. **444**, 185 (1996).
[7] B. Yuan and W. Sharpe, Jr., Exp. Tech. **21**, 32 (1997).
[8] K. Kamitani, M. Grimsditch, J. C. Nipko, C.-K. Loong, M. Okada, and I. Kimura, J. Appl. Phys. **82**, 3152 (1997).
[9] P. Djemia, Ph.D. thesis, Université Paris Nord, France, 1998.
[10] P. Djemia, C. Dugautier, T. Chauveau, M. I. De Barros, and L. Vandenbulcke, J. Appl. Phys. **90**, 3771 (2001).
[11] P. Moch, P. Djemia, and F. Ganot, Vide (Société Française du Vide, Paris) **301**, 565 (2001).
[12] K. M. Jackson, G. F. Dirras, R. L. Edwards, and W. N. Sharpe, Jr., in *Proceedings of the SEM Annual Conference*, edited by A. Shukla, R. M. French, A. Andonian, and K. M. Ramsay (Society for Experimental Mechanics Inc., Bethel, CT, 2002) pp. 99-101.
[13] G. F. Dirras, P. Djemia, T. Chauveau, H. S. Cho, K. M. Jackson, G. Coles, and K. J. Hemker, Recent Res. Devel. Mat. Sci. Eng. **2**, 79 (2003).
[14] D. W. Feldman, J. H. Parker, Jr., J. W. Choyke, and L. Patrick, Phys. Rev. B **173**, 787 (1968).
[15] W. R. L. Lambrecht, B. Segall, M. Methfessel, and M. van Schilfgaarde, Phys. Rev. B **44**, 3685 (1991).
[16] K. Karch, P. Pavone, W. Windl, O. Schütt, and D. Strauch, Phys. Rev. B **50**, 17054 (1994).
[17] W. Li and T. Wang, Phys. Rev. B **59**, 3993 (1999).
[18] J. F. Nye, *Physical Properties of Crystals* (Clarendon, Oxford, 1957), Chap. VIII.
[19] J. Turley and G. Sines, J. Phys. D **4**, 264 (1971).
[20] B. Hillebrands, S. Lee, G. I. Stegeman, H. Cheng, J. E. Potts, and F. Nizzoli, Phys. Rev. Lett. **60**, 832 (1988).
[21] B. Schultrich, H.-J. Scheibe, G. Grandremy, D. Drescher, and D. Schneider, Diamond Relat. Mater. **5**, 914 (1996).
[22] M. J. P. Musgrave, *Crystal Acoustic* (Holden Day, San Francisco, 1970).
[23] J. B. Wachtman and D. G. Lam, J. Am. Ceram. Soc. **42**, 254 (1959).
[24] B. P. Pandey and B. Dayal, Phys. Status Solidi B **58**, K53 (1973).